ELSEVIER

www.elsevier.nl/locate/jorganchem

Journal of Organometallic Chemistry 595 (2000) 276–284

Journal of Organometallic Chemistry

Reactions of $[Pt_2(\mu\text{-}S)_2(PPh_3)_4]$ with Group 6 and 7 metal carbonyls; crystal structure of the apparently unsaturated heterometallic complex $[Pt_2Re(\mu_3\text{-}S)_2(PPh_3)_4(CO)_3]^+$

Huang Liu [a], Chenghua Jiang [a], Jeremy S.L. Yeo [a], Kum Fun Mok [a], Ling Kang Liu [b], T.S. Andy Hor [a,1], Yaw Kai Yan [c,*]

[a] *Department of Chemistry, Faculty of Science, National University of Singapore, Kent Ridge, Singapore 119260, Singapore*
[b] *Institute of Chemistry, Academia Sinica, Taipei 11529, Taiwan, ROC*
[c] *Division of Chemistry, National Institute of Education, Nanyang Technological University, 469 Bukit Timah Road, Singapore 259756, Singapore*

Received 1 September 1999; received in revised form 27 September 1999; accepted 4 October 1999

Abstract

Reaction of $[Pt_2(\mu\text{-}S)_2(PPh_3)_4]$ (**1**) with a mixture containing $[Re_2(CO)_{10}]$, $Me_3NO{\cdot}2H_2O$ and MeOH at room temperature affords an oxidative methoxylation complex, $[Pt_2Re_2(\mu\text{-}OMe)_2(\mu_3\text{-}S)_2(PPh_3)_4(CO)_6]$ (**2**), and a Pt–Re heterometallic salt, $[Pt_2Re(\mu_3\text{-}S)_2(PPh_3)_4(CO)_3]^+[Re_3(\mu_3\text{-}OMe)(\mu\text{-}OMe)_3(CO)_9]^-$ (**3a**). The core of the cation of **3a** comprises a $\{Pt_2ReS_2\}$ trigonal bipyramidal 'cluster' with weak Pt–Re bonding interactions and an apparently unsaturated Re(I) atom. The $[BF_4]^-$ salt of this cation, **3b**, can be prepared by the reaction of **1** with $[Re(CO)_5(H_2O)][BF_4]$, and the Mn analogue, $[Pt_2Mn(\mu_3\text{-}S)_2(PPh_3)_4(CO)_3][BF_4]$ (**4**), can be similarly synthesised using $[Mn(FBF_3)(CO)_5]$. Addition of **1** to $[M(I)_2(CO)_3(NCMe)_2]$ (M = Mo, W) is accompanied by iodide migration to give the salts $[Pt_2M(\mu_3\text{-}S)_2I(PPh_3)_4(CO)_4][M(I)_3(CO)_4]$ (M = Mo, **5**; W, **6a**). With $[Mo(CO)_4(NCMe)_2]$, **1** undergoes reductive carbonylation and desulfurization to give $[Pt_2(\mu\text{-}S)(PPh_3)_3(CO)]$ (**7**). The above reactions represent the first examples of **1** as a metalloligand towards carbonyl complexes of the less electron-rich transition metals, and demonstrate that addition reactions of **1** can be complicated by ligand dissociation, ligand migration, or reductive desulphurization. The crystal structures of compounds **3a** and **3b** were determined.

Keywords: Platinum; Sulfide; Rhenium; Tungsten; Metalloligand; Heterometallic

1. Introduction

Extensive studies have shown that $[Pt_2(\mu\text{-}S)_2(PPh_3)_4]$ (**1**) is a versatile precursor in the rational synthesis of heterometallic multinuclear platinum sulfide complexes [1–7]. The nucleophilicity and adjustable orientations of the sulfur lone pairs in **1** make the complex a powerful Lewis base that supports a wide variety of coordination geometries of the heterometals.

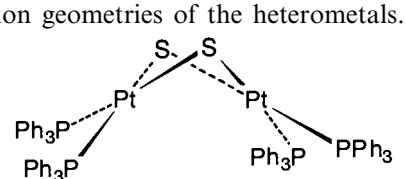

1

Multinuclear aggregates with three to six metal centres have been synthesised by the reaction of **1** with a variety of electron-rich (d^8 and d^{10}) metal fragments, e.g. Cu(I), Ag(I), Au(I), Pd(II), Pt(II), and Rh(I) [1–6]. There was no apparent initiative for similar experimentation to be carried out with the earlier metals as **1** was not expected to behave differently towards these metals. Using some representative Group 6 ($[Mo(I)_2(CO)_3(NCMe)_2]$, $[W(I)_2(CO)_3(NCMe)_2]$, and $[Mo(CO)_4(NCMe)_2]$) and Group 7 ($[Re_2(CO)_{10}]$, $[Re(CO)_5(H_2O)][BF_4]$ and $[Mn(FBF_3)(CO)_5]$) metal carbonyls as substrates, we demonstrate, however, that in the course of the formation of heterometallic Lewis acid/base adducts with **1**, complications such as ligand dissociation and migration, ion-pair formation or reductive desulfurization can occur, which lead to some unexpected products. This is best illustrated by the reactions of **1** with

* Corresponding author. Fax: +65-469-89-52.
E-mail address: ykyan@nie.edu.sg (Y.K. Yan)
[1] Also corresponding author.

0022-328X/00/$ - see front matter
PII: S0022-328X(99)00640-3

$[M(I)_2(CO)_3(NCMe)_2]$ (M = Mo, W) and $[Re_2(CO)_{10}]$/Me_3NO, which lead to the isolation of $[Pt_2MI(PPh_3)_4(CO)_4(\mu_3\text{-}S)_2][M(I)_3(CO)_4]$ and $[Pt_2Re(\mu_3\text{-}S)_2(PPh_3)_4(CO)_3][Re_3(\mu_3\text{-}OMe)(\mu\text{-}OMe)_3(CO)_9]$, respectively. The formation of these heterometallic salts from ligand migration suggests that the metalloligand chemistry of **1** is rich and that the current view of its reactivity being confined to direct adduct formation is too simplistic.

2. Results and discussion

2.1. Reaction of $[Pt_2(\mu\text{-}S)_2(PPh_3)_4]$ (1) with Group 7 metal carbonyls

Oxidative decarbonylation of $[Re_2(CO)_{10}]$ by Me_3NO in the presence of MeOH at room temperature (r.t.) followed by the addition of **1** results in $[Pt_2Re_2(\mu\text{-}OMe)_2(\mu_3\text{-}S)_2(PPh_3)_4(CO)_6]$ (**2**) and $[Pt_2Re(\mu_3\text{-}S)_2(PPh_3)_4(CO)_3][Re_3(\mu_3\text{-}OMe)(\mu\text{-}OMe)_3(CO)_9]$ (**3a**). The identity of **2**, which can be thought of as comprising two $Re(CO)_3$ units bridged by two methoxo groups and one dithio ligand $[Pt_2(\mu\text{-}S)_2(PPh_3)_4]$, is deduced from its spectroscopic data, and by the analogy between its synthesis procedure and that of the analogous diphosphine-bridged complexes $[Re_2(\mu\text{-}OMe)_2(\mu\text{-}PP)(CO)_6]$ (PP = diphosphine) [8].

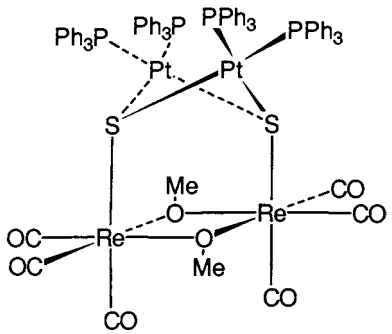

2

The IR (ν_{CO}) spectrum of complex **2** is very similar to those of the latter [8]. Its ^{1}H-NMR spectrum shows a complex resonance at 7.19–7.46 ppm, which is attributed to the phenyl protons of the PPh_3 ligands, and a singlet signal at 4.22 ppm, which is assigned to the bridging methoxo protons. The integration ratio of ca. 10:1 confirms the presence of four PPh_3 ligands per two methoxo groups. The $^{31}P\{^1H\}$ spectrum shows a sharp signal at 17.5 ppm which is flanked symmetrically by a pair of characteristic ^{195}Pt satellites ($^1J(^{31}P\text{–}^{195}Pt) = 3255$ Hz). This is consistent with the presence of Pt-bonded phosphines that are chemically equivalent. That complex **2** is a non-electrolyte in solution is also consistent with its proposed formula. Complex **2** is likely to be formed via direct attack of **1** on the intermediate $[Re_2(CO)_8(\mu\text{-}OMe)_2]$, the presence of which in the $[Re_2(CO)_{10}]$–Me_3NO–MeOH mixture has been discussed in our earlier work [9,10].

Complex **3a** displays a conductivity in MeOH solution typical of that of a 1:1 electrolyte in MeOH [11]. Its $^{31}P\{^1H\}$-NMR spectrum indicates that the phosphine groups are Pt-bound and chemically equivalent. The ^{1}H-NMR spectrum shows the phenyl peaks in the 7.2–7.5 ppm region. Two singlets attributed to the $\mu\text{-}OCH_3$ and $\mu_3\text{-}OCH_3$ protons are also observed at 4.25 and 4.52 ppm, respectively. The integration ratio of ca. 20:3:1 confirms the presence of four PPh_3 ligands and three $\mu\text{-}OCH_3$ groups per $\mu_3\text{-}OCH_3$ group.

2.2. Crystal structure of $[Pt_2Re(\mu_3\text{-}S)_2(PPh_3)_4(CO)_3][Re_3(\mu_3\text{-}OMe)(\mu\text{-}OMe)_3(CO)_9]$ (3a)

Single-crystal X-ray diffraction analysis revealed **3a** to be a salt with a heterometallic $RePt_2$ cation and a homometallic trirhenium anion (Figs. 1 and 2). The cation is best viewed as a sulfide-bicapped heterometallic $\{Pt_2Re\}$ triangle in a trigonal bipyramidal framework. It is a 48-electron aggregate with an apparently unsaturated 16-electron, five-coordinate Re(I) core. Although the quality of the structural data is not sufficiently high to allow a detailed bonding analysis, some geometrical characteristics are significant and worthy of mention. While the Pt···Pt separation (3.275(5) Å) is typically non-bonding [12], the Pt···Re distances (3.067(6) and 3.099(6) Å) are within the range for weak bonding (cf. the Pt–Re bond lengths of $[PtRe_3(CO)_{14}(\mu\text{-}H)_3]$ [13] fall in the range of 2.769(1) to 3.067(1) Å). With the Pt and Re atoms in close contact, we can propose a donation of two electrons from the totally

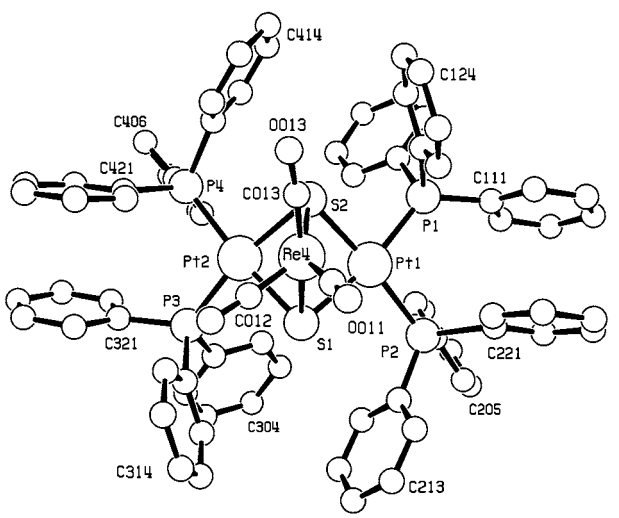

Fig. 1. Structure of the cation of $[Pt_2Re(\mu_3\text{-}S)_2(PPh_3)_4(CO)_3][Re_3(\mu\text{-}OMe)_3(\mu_3\text{-}OMe)(CO)_9]$ (**3a**). Key bond lengths (Å): Pt(1)···Re(4) 3.099(6), Pt(2)···Re(4) 3.067(6), Pt(1)–S(1) 2.38(2), Pt(1)–S(2) 2.31(2), Pt(2)–S(1) 2.38(2), Pt(2)–S(2) 2.38(2), Re(4)–S(1) 2.40(2), Re(4)–S(2) 2.40(2).

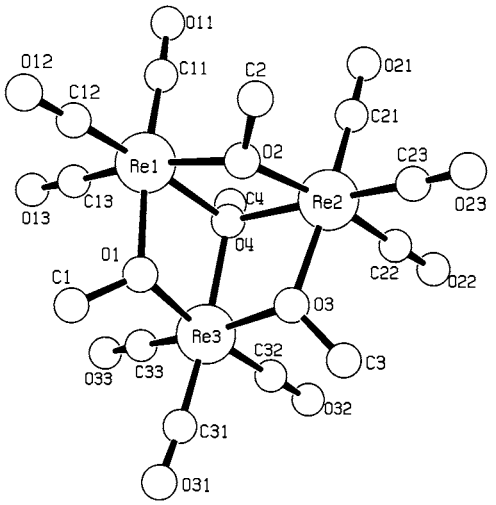

Fig. 2. Structure of the anion of $[Pt_2Re(\mu_3\text{-}S)_2(PPh_3)_4(CO)_3][Re_3(\mu\text{-}OMe)_3(\mu_3\text{-}OMe)(CO)_9]$ (**3a**).

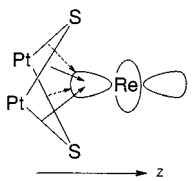

Fig. 3. Proposed donation of electron density from the Pt–S σ-bonds to the empty d_{z^2} orbital of Re in the cation $[Pt_2Re(\mu_3\text{-}S)_2(PPh_3)_4(CO)_3]^+$.

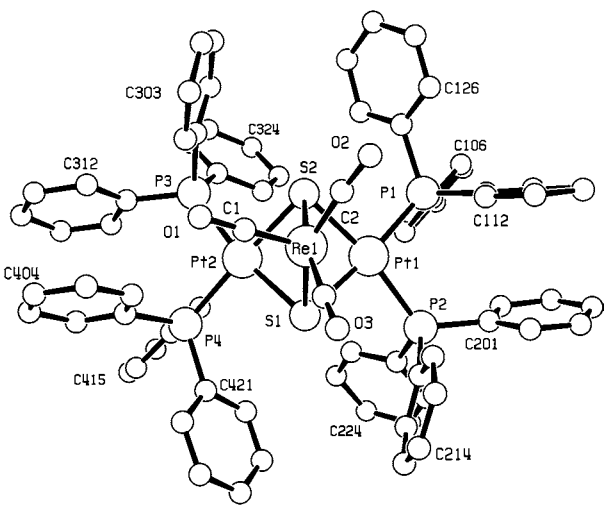

Fig. 4. Structure of the cation of $[Pt_2Re(\mu_3\text{-}S)_2(PPh_3)_4(CO)_3][BF_4]$ (**3b**).

symmetric linear combination of σ(Pt–S) orbitals to the empty d_{z^2} orbital of Re (Fig. 3). This effectively gives rise to an 18-electron Re(I) centre. The local geometry of Re(I) can hence be described as a 'piano stool' with the carbonyls serving as the three legs and Pt_2S_2 as the seat. This explanation of bonding in **3a** is analogous to that proposed for the cluster $[Pt_3\{\mu_3\text{-}Re(CO)_3\}(\mu\text{-}dppm)_3]^+$, where the Re atom achieves its 18-electron configuration by accepting electrons from the three Pt–Pt bonds of the $[Pt_3(\mu\text{-}dppm)_3]$ fragment [14].

It is nevertheless peculiar that the Re(I) centre chooses to opt for a coordination sphere with three strong Re–CO bonds and two strong Re–S bonds, plus two weak Pt–Re interactions, rather than the expected octahedral configuration of $\{Re(CO)_4(S\text{–}S)\}$ [S–S = $Pt_2(\mu\text{-}S)_2(PPh_3)_4$]. This coordinative unsaturation of the Re centre may reflect the steric demand of the bulky metallo ligand **1** on the Re(I) core.

The anion in **3a**, $[Re_3(\mu_3\text{-}OMe)(\mu\text{-}OMe)_3(CO)_9]^-$, has previously been structurally characterised as its $[NEt_4]^+$ salt [15]. It consists of a Re_3 triangle held together by one face-capping and three edge-bridging methoxo groups, with no Re–Re bonds.

2.3. Mechanism for the formation of compound *3a*

Whilst the precise mechanism for the formation of **3a** is unknown, the cation possibly arises from the displacement of the methoxide group and one CO ligand of $[Re(CO)_4(OMe)]$ by $[Pt_2(\mu\text{-}S)_2(PPh_3)_4]$. The presence of the intermediate $[Re(CO)_4(OMe)]$ in the $[Re_2(CO)_{10}]$–Me_3NO–MeOH reaction mixture has been previously discussed [16]. The $[Re_3(\mu_3\text{-}OMe)(\mu\text{-}OMe)_3(CO)_9]^-$ anion would then be formed from the aggregation of the free methoxide with three $[Re(CO)_4(OMe)]$ fragments, with concomitant loss of CO. There is no evidence that **2** and **3a** are directly related mechanistically.

2.4. Synthesis and crystal structure of $[Pt_2Re(\mu_3\text{-}S)_2(PPh_3)_4(CO)_3][BF_4]$ (*3b*)

The poor quality of the structural data for **3a** is due mainly to poor crystal quality and disorder in the $[Re_3(\mu_3\text{-}OMe)(\mu\text{-}OMe)_3(CO)_9]^-$ anion. Despite repeated attempts, we were unable to grow better crystals of **3a**. Attempts were thus made to exchange the $[Re_3(\mu_3\text{-}OMe)(\mu\text{-}OMe)_3(CO)_9]^-$ anion with $[PF_6]^-$, with the hope that the hexafluorophosphate salt of $[Pt_2Re(\mu_3\text{-}S)_2(PPh_3)_4(CO)_3]^+$ would be easier to crystallise. Moreover, replacing the disordered $[Re_3(\mu_3\text{-}OMe)(\mu\text{-}OMe)_3(CO)_9]^-$ anion, which contains three very heavy Re atoms, by an anion comprising much lighter atoms, should improve the refinement of the atomic coordinates of the $[Pt_2Re(\mu_3\text{-}S)_2(PPh_3)_4(CO)_3]^+$ cation, which is the focus of our attention. We have not been able, however, to prepare the hexafluorophosphate salt of $[Pt_2Re(\mu_3\text{-}S)_2(PPh_3)_4(CO)_3]^+$ by metathesis with $[NH_4][PF_6]$.

An alternative strategy was to synthesise the tetrafluoroborate salt of $[Pt_2Re(\mu_3\text{-}S)_2(PPh_3)_4(CO)_3]^+$ by reacting $[Pt_2(\mu\text{-}S)_2(PPh_3)_4]$ with $[Re(CO)_5(H_2O)][BF_4]$. This strategy turned out to be successful, and gave a

52% yield of $[Pt_2Re(\mu_3\text{-}S)_2(PPh_3)_4(CO)_3][BF_4]$ (**3b**) as red–orange crystals.

The crystal structure of **3b** (Fig. 4) confirms the deductions regarding the $[Pt_2Re(\mu_3\text{-}S)_2(PPh_3)_4(CO)_3]^+$ cation drawn from the crystal structure of **3a**. In addition, the better quality of the structural data for **3b** allows a more detailed analysis of the geometry of the cation. The $\{Pt_2S_2\}$ ring is hinged at an angle of 130° (between two PtS_2 planes). The Pt···Pt (3.255 Å) and S···S (3.080 Å) distances are typically non-bonding [12]. The Pt···Re distances are unequal, with the Re atom significantly closer to Pt(1) (3.0668(9) Å) than Pt(2) (3.1678(8) Å). This is probably due to repulsion between Pt(2) and the carbonyl group {C(1)–O(1)}. Both the Pt···Re distances are, however, short enough to be consistent with the proposed weak Pt···Re bonding interaction.

The Re–S(2) bond [2.452(3) Å] is slightly longer than the Re–S(1) bond (2.437(3) Å), probably due to the competition for Re d-orbital interaction between S(2) and the carbonyl group *trans* to it {C(3)–O(3)}. Correspondingly, the Re–C(3) bond is also the longest of the three Re–CO bonds (Table 1). The average Re–CO bond length (1.862(1) Å) is much shorter than that in other *fac*-$\{Re^I(CO)_3\}$ units (ca. 1.90 Å) [15,17]. The range of IR ν_{CO} frequencies for **3b** (2012–1896 cm^{-1}) is; however, similar to that for the complexes $[Re_2(\mu\text{-}OR)_2(\mu\text{-dppf})(CO)_6]$ [R = H, Me, Et, Ph; dppf = 1,1′-bis(diphenylphosphino)ferrocene] (2027–1887 cm^{-1}), which also contain *fac*-$\{Re^I(CO)_3\}$ units [9,15]. These observations suggest that the Re–CO backbonding in **3b** is quite strong, and that the Re atom is not electron deficient.

Judging from the Re–Pt and Re–S distances, the Pt(1)–S(1) bond is the nearest Pt–S bond to the Re atom, and is expected to interact most strongly with it. Correspondingly, the Pt(1)–S(1) bond is the longest of the Pt–S bonds (Table 1). This is consistent with the proposed donation of electron density from the Pt–S bonds to the Re atom.

Table 1
Selected bond lengths (Å) and angles (°) for compound **3b**

Bond lengths			
Pt(1)–Re(1)	3.0668(9)	Re(1)–C(1)	1.834(1)
Pt(2)–Re(1)	3.1678(8)	Re(1)–C(2)	1.856(1)
Pt(1)–S(1)	2.384(3)	Re(1)–C(3)	1.895(1)
Pt(1)–S(2)	2.355(4)	C(1)–O(1)	1.230(1)
Pt(2)–S(1)	2.359(4)	C(2)–O(2)	1.209(1)
Pt(2)–S(2)	2.368(3)	C(3)–O(3)	1.168(1)
Re(1)–S(1)	2.437(3)		
Re(1)–S(2)	2.452(3)		
Bond angles			
S(1)–Pt(1)–S(2)	81.1(1)	C(1)–Re(1)–S(1)	121.7(6)
S(1)–Pt(2)–S(2)	81.3(1)	C(2)–Re(1)–S(1)	152.8(5)
Pt(1)–S(1)–Pt(2)	86.7(1)	C(3)–Re(1)–S(1)	95.3(5)
Pt(1)–S(2)–Pt(2)	87.1(1)	C(1)–Re(1)–S(2)	109.2(4)
Pt(1)–Re(1)–Pt(2)	62.91(2)	C(2)–Re(1)–S(2)	94.8(5)
S(1)–Re(1)–S(2)	78.1(1)	C(3)–Re(1)–S(2)	166.8(6)
C(1)–Re(1)–Pt(1)	155.1(4)	C(1)–Re(1)–C(2)	85.5(8)
C(2)–Re(1)–Pt(1)	106.1(5)	C(1)–Re(1)–C(3)	84.0(7)
C(3)–Re(1)–Pt(1)	118.2(5)	C(2)–Re(1)–C(3)	86.0(7)
C(1)–Re(1)–Pt(2)	93.9(5)	O(1)–C(1)–Re(1)	176(1)
C(2)–Re(1)–Pt(2)	140.0(6)	O(2)–C(2)–Re(1)	175(1)
C(3)–Re(1)–Pt(2)	133.8(5)	O(3)–C(3)–Re(1)	178(2)

Table 2
Infrared carbonyl absorption data (KBr discs) of complexes **5**, **6a** and **6b**

Complex	ν(CO) (cm^{-1})
$[Pt_2Mo(\mu_3\text{-}S)_2I(PPh_3)_4(CO)_4]^+$-$[Mo(I)_3(CO)_4]^-$ (**5**)	2063(s), 2034(m), 2010(vs), 1983(s), 1942(s), 1926(vs), 1881(s), 1870(s)
$[Pt_2W(\mu_3\text{-}S)_2I(PPh_3)_4(CO)_4]^+$-$[W(I)_3(CO)_4]^-$ (**6a**)	2062(s), 2018(m, sh), 2000(vs), 1986(vs), 1960(m), 1923(vs), 1911(s), 1868(s)
$[Pt_2W(\mu_3\text{-}S)_2I(PPh_3)_4(CO)_4][PF_6]$ (**6b**)	2067(m), 2000(vs), 1961(m), 1927(s)

2.5. Reaction of $[Pt_2(\mu\text{-}S)_2(PPh_3)_4]$ (**1**) with $[Mn(FBF_3)(CO)_5]$

Reaction of **1** with $[Mn(FBF_3)(CO)_5]$, generated in situ by the reaction of $AgBF_4$ with $MnBr(CO)_5$, afforded a blue–violet product analysed as $[Pt_2Mn(\mu_3\text{-}S)_2(PPh_3)_4(CO)_3][BF_4]\cdot 2H_2O$ (**4**). The ^{31}P-NMR and IR (ν_{CO}) spectra of compound **4** are very similar to those of **3b**, its Re analogue. Compound **4** is rather air-sensitive in solution, however, decomposing within 1 day at r.t. to a yellow product, which is presently unidentified.

2.6. Reaction of $[Pt_2(\mu\text{-}S)_2(PPh_3)_4]$ (**1**) with Group 6 metal carbonyls

Reactions of **1** with $[M(I)_2(CO)_3(NCMe)_2]$ (M = Mo, W) in a 1:1 molar ratio in THF are sluggish and leave behind substantial portions of **1** unreacted. In a molar ratio of 1:2, the reactions take place readily to give clear red–brown solutions from which $[Pt_2M(\mu_3\text{-}S)_2I(PPh_3)_4(CO)_4][M(I)_3(CO)_4]$ (M = Mo, **5**; W, **6a**) can be isolated. These are examples of high-coordinate M(II) complexes, which have been well-studied by Baker [18–20] and other researchers [21–26]. Attempts to grow single crystals of compounds **5** and **6a** suitable for X-ray diffraction studies have been unsuccessful. The identities of these compounds can, however, be deduced from their spectroscopic, conductivity and elemental analysis data (see Section 3). The molar conductivities of **5** and **6a** are consistent with the compounds being 1:1 electrolytes [11]. Both **5** and **6a** show eight terminal carbonyl absorption bands in the range 1868–2063 cm^{-1} in their IR spectra (Table 2). The large number of carbonyl bands over a large absorption

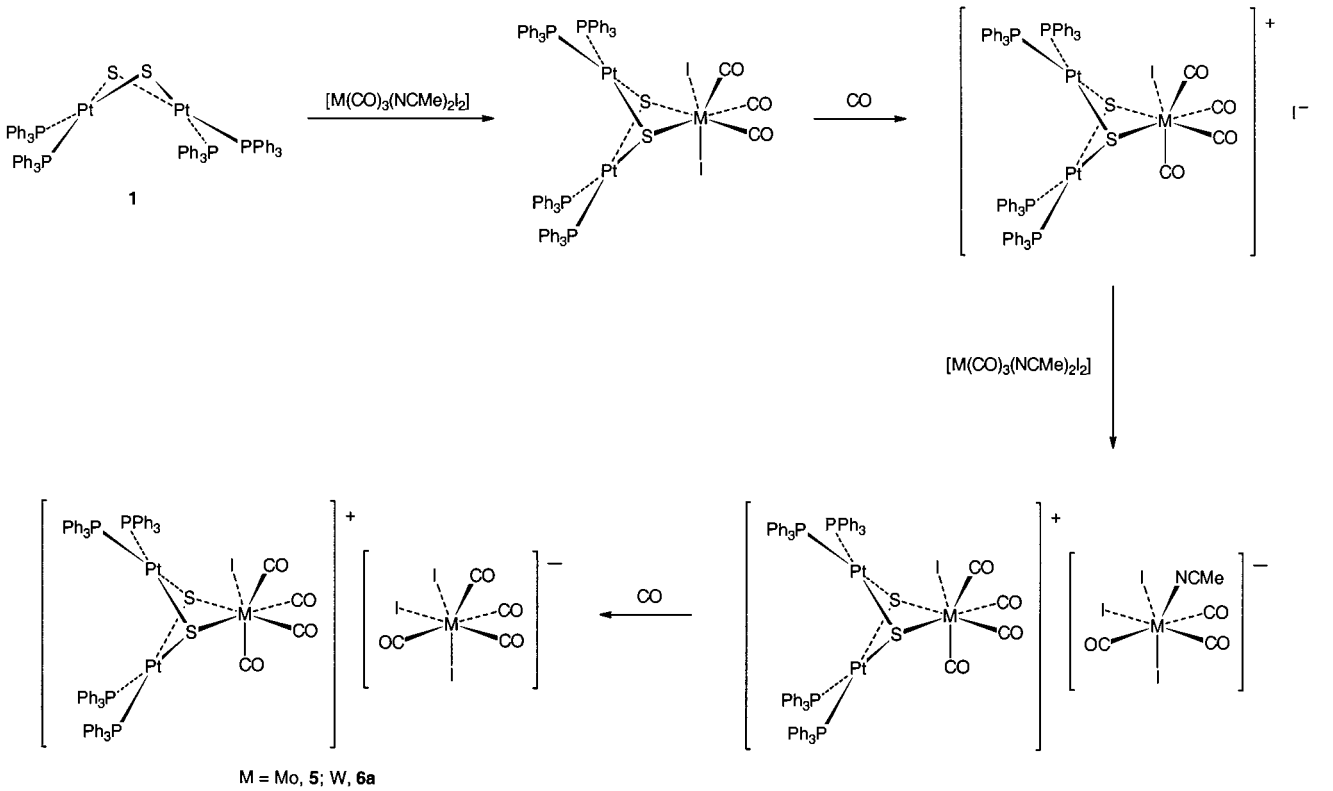

Scheme 1.

region is consistent with a salt with carbonyls on both the cation and anion. The isomorphic nature of both complexes is indicated by their similar IR bands. The absence of nitrile absorptions in the ν(C≡N) region (2200–2400 cm^{-1}) confirms the complete substitution of the MeCN ligands. Anion exchange can be carried out on **6a** with NH_4PF_6 in MeOH solution to give $[Pt_2W(\mu_3\text{-}S)_2I(PPh_3)_4(CO)_4][PF_6]$ (**6b**) as a red–brown precipitate. Similar treatment of **5** with NH_4PF_6, however, did not yield any precipitate of $[Pt_2Mo(\mu_3\text{-}S)_2I(PPh_3)_4(CO)_4][PF_6]$. The presence of the uncoordinated $[PF_6]^-$ anion in **6b** is verified by a strong IR band at 837 cm^{-1}. Compared to the eight carbonyl absorptions of **6a**, only four CO bands remain in the IR spectrum of **6b**. This is consistent with the presence of four carbonyl groups in both cation and anion of **6a**, respectively. The $^{31}P\{^1H\}$-NMR spectra of **5** and **6a**, which give a single resonance with characteristic ^{195}Pt coupling, indicate that the phosphines are Pt-coordinated and chemically equivalent, as they would be if the $[Pt_2(\mu\text{-}S)_2(PPh_3)_4]$ ligand is coordinated to the Group 6 metal as a chelate via the two sulfur atoms. Elemental analysis data for **5**, **6a** and **6b** are all in good agreement with the proposed formulae of the compounds. Further support for the proposed identities of **5** and **6a** is obtained from the analogy between the reactions leading to these compounds and the reaction of $[M(I)_2(CO)_3(NCMe)_2]$ with 3,3,7,7,11,11,15,15-octamethyl-1,5,9,13-tetrathiacyclohexadecane ($Me_8[16]aneS_4$) to form $[MI(CO)_3\{\eta^3\text{-}(Me_8[16]aneS_4)\}][M(I)_3(CO)_4]$ (M = Mo, W) [18a].

The proposed mechanism for the formation of **5** and **6a** is shown in Scheme 1. Addition of **1** to $[M(I)_2(CO)_3(NCMe)_2]$ gives an addition product that rapidly ionises through iodide dissociation in a donor solvent. Iodide substitution of the labile MeCN on $[M(I)_2(CO)_3(NCMe)_2]$ yields an ion pair which adds CO (from $[M(I)_2(CO)_3(NCMe)_2]$) to give the final products. This is analogous to the mechanism proposed for the reaction of $[M(I)_2(CO)_3(NCMe)_2]$ with $Me_8[16]aneS_4$ to form $[MI(CO)_3\{\eta^3\text{-}(Me_8[16]aneS_4)\}][M(I)_3(CO)_4]$ (M = Mo, W) [18a]. With an 18-electron capped octahedral Mo^{II}/W^{II}, no Pt–Pt or Mo/W–Pt bond is envisaged for the cations of compounds **5** and **6a**.

Complexes **5** and **6a** are air-stable solids, but their solutions (in MeOH or acetone) are stable only when stored under argon. The complexes decompose readily in CH_2Cl_2 to regenerate **1**, which subsequently reacts with CH_2Cl_2 to give $[Pt_2(\mu\text{-}S)(\mu\text{-}SCH_2Cl)(PPh_3)_4]Cl$ and finally $[Pt(SCH_2Cl)_2(PPh_3)_2]$ [27]. The latter is verified by $^{31}P\{^1H\}$-NMR analysis.

Complex **1** does not give the expected product, $[Pt_2Mo(\mu_3\text{-}S)_2(PPh_3)_4(CO)_4]$ with $[Mo(CO)_4(NCMe)_2]$. Instead, $[Pt_2(\mu\text{-}S)(PPh_3)_3(CO)]$ (**7**) [28,29] is formed (in 15% yield), and no Mo-containing product can be isolated.

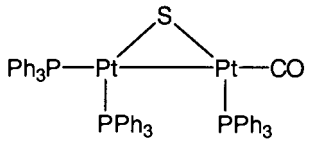

7

Formation of **7** from **1** signifies a reductive desulfurisation reaction, which has been discussed elsewhere [28]. The different behaviour of **1** towards $[Mo(I)_2(CO)_3(NCMe)_2]$ and $[Mo(CO)_4(NCMe)_2]$ suggests that the oxidation state of the heterometal is an important factor governing the reaction pathway.

3. Experimental

3.1. Materials and methods

All reactions were performed under argon. All solvents were analytical grade and were distilled and degassed by argon before use. $[Pt_2(\mu\text{-}S)_2(PPh_3)_4]$ [30], $[M(I)_2(CO)_3(NCMe)_2]$ (M = Mo, W) [19a] and $[Mo(CO)_4(NCMe)_2]$ [31] were synthesised according to literature methods. Elemental analyses were conducted in the Microanalytical Laboratory in the Department of Chemistry of the National University of Singapore. Infrared spectra were taken on a Perkin–Elmer 1600 FTIR spectrophotometer. Conductivity was measured by using a STEM Conductivity 1000 meter. ^{1}H- and $^{31}P\{^1H\}$-NMR spectra were run on a Bruker ACF 300 spectrometer at 298 K. Chemical shifts are quoted in ppm downfield of Me_4Si and 80% H_3PO_4, respectively.

3.2. Syntheses of $[Pt_2Re_2(PPh_3)_4(CO)_6(\mu\text{-}OMe)_2(\mu_3\text{-}S)_2]$ (**2**) and $[Pt_2Re(PPh_3)_4(CO)_3(\mu_3\text{-}S)_2][Re_3(CO)_9(\mu\text{-}OMe)_3(\mu_3\text{-}OMe)]$ (**3a**)

A solution of $Me_3NO{\cdot}2H_2O$ (0.062 g, 0.56 mmol) in THF–MeOH (1:1, 20 cm^3) was transferred with stirring into a solution of $Re_2(CO)_{10}$ (0.151 g, 0.23 mmol) in THF (10 cm^3) at r.t. After 4 h complex **1** (0.075 g, 0.05 mmol, as a solid) was introduced into the reaction mixture. The suspension dissolved in a period of 30 min to give a clear golden-yellow solution. Stirring was continued for 3 h to ensure complete reaction. All solvent was removed under vacuum and the residue was crystallized in ether–hexane. In 3–4 days a small amount of yellowish brown clumps of tiny crystals of **2** was formed on the wall of the flask (yield 0.010 g, 10% based on Pt) together with a chrome-yellow precipitate of **3a**·at the bottom of the flask (yield 0.029 g, 21% based on Pt). Crystals of **2** were manually separated from the precipitate of **3a**. The latter was then recrystallised from ether–hexane to give orange crystals. Both **2** and **3a** are air sensitive in solution. For **2**: Anal. Calc. for $C_{80}H_{66}O_8P_4Pt_2Re_2S_2$: C, 45.6; H, 3.1; P, 5.9; Re, 17.7; S, 3.0. Found: C, 45.2; H, 3.0; P, 5.5; Re, 17.2; S, 2.9%. ν(CO) (CH_2Cl_2) 2007 s, 1993 m, 1914 m (sh), 1887 vs, 1879 s (sh) cm^{-1}. δ_H (acetone-d_6) 4.22 (s, 6H, μ-OCH_3) and 7.19–7.46 (m, 60H, Ph); δ_P (acetone-d_6) 17.5 (t, $^1J(^{31}P\text{–}^{195}Pt) = 3255$ Hz); for **3a**·Et_2O: Anal. Calc. for $C_{92}H_{82}O_{17}P_4Pt_2Re_4S_2$: C, 39.7; H, 3.0; P, 4.4; Pt, 14.0; Re, 26.8; S, 2.3. Found: C, 39.6; H, 3.0; P, 4.5; Pt, 12.9; Re, 24.7; S, 2.2%. Λ_m (10^{-3} M, MeOH) 74 ohm^{-1} cm^2 mol^{-1}. ν(CO) (acetone) 2011 w, 2004 s, 1916 m, 1893 vs, 1876 sh cm^{-1}. δ_H (acetone-d_6) 4.25 (s, 9H, μ-OCH_3), 4.52 (s, 3H, μ_3-OCH_3) and 7.2–7.5 (m, 60H, Ph); δ_P (acetone-d_6) 17.5 (t, $^1J(^{31}P\text{–}^{195}Pt) = 3263$ Hz).

3.3. Synthesis of $[Pt_2Re(PPh_3)_4(CO)_3(\mu_3\text{-}S)_2][BF_4]$ (**3b**)

Solid $[Pt_2(\mu\text{-}S)_2(PPh_3)_4]$ (0.089 g, 0.06 mmol) was added with stirring to a solution of $[Re(CO)_5(H_2O)][BF_4]$ [32] (0.024 g, 0.06 mmol) in acetone (30 cm^3). The orange suspension dissolved to give a clear orange solution after 4 h. Stirring was continued for 1 day to ensure complete reaction. The acetone solution was allowed to vaporise slowly in air. After 2 days, reddish-orange crystals of **3b** appeared (yield 0.057 g, 52%). Anal. Calc. for $C_{75}H_{60}F_4O_3P_4Pt_2ReS_2$: C, 48.4; H, 3.3; P, 6.7; Pt, 21.0; Re, 10.0; S, 3.5. Found: C, 47.5; H, 3.0; P, 6.2; Pt, 20.7; Re, 11.2; S, 3.9%. ν(CO) (acetone) 2012 s, 1916 m, 1896 m cm^{-1}. δ_P (acetone-d_6) 17.4 (t, ^1J(P–Pt) 3257 Hz). The carbon analysis was consistently lower than the calculated value, despite satisfactory agreement for the other elemental analyses, possibly due to the formation of a small amount of refractory carbides (rhenium, platinum or boron carbides) during combustion analysis.

3.4. Reaction of $[Pt_2(\mu\text{-}S)_2(PPh_3)_4]$ (**1**) with $[Mn(FBF_3)(CO)_5]$

Solid $AgBF_4$ (0.015 g, 0.08 mmol) was added to a stirred solution of $MnBr(CO)_5$ (0.016 g, 0.06 mmol) in CH_2Cl_2 (30 cm^3). The mixture was shielded from light and allowed to react for 3 h, after which it was filtered under argon into another Schlenk flask. The CH_2Cl_2 solvent was removed from the yellow filtrate under vacuum, and the residue was redissolved in 30 cm^3 of acetone. Solid $[Pt_2(\mu\text{-}S)_2(PPh_3)_4]$ (0.087 g, 0.06 mmol) was then added to the acetone solution, giving an orange suspension. The suspension turned dark green a few minutes later and eventually grey after 5 h. The mixture was stirred for a total of 24 h and then filtered. The blue–violet filtrate was concentrated under vacuum and treated with deionised water to precipitate the product. The blue–violet powder formed was washed with deionised water, followed by ether, and dried by

suction. It was analysed as $[Pt_2Mn(\mu_3\text{-}S)_2(PPh_3)_4(CO)_3][BF_4]\cdot 2H_2O$ (**4**) (0.033 g, 31%). Anal. Calc. for $C_{75}H_{64}BF_4O_5P_4Pt_2MnS_2$: C, 51.0; H, 3.7. Found: C, 50.8; H, 3.6%. ν(CO) (acetone) 2010 vs, 1931 m, 1908 m cm^{-1}. δ_P (acetone-d_6) 18.8 (t, ^1J(P–Pt) = 3258 Hz).

3.5. Synthesis of $[Pt_2Mo(\mu_3\text{-}S)_2I(PPh_3)_4(CO)_4][Mo(I)_3(CO)_4]$ (5)

Solid $[Pt_2(\mu\text{-}S)_2(PPh_3)_4]$ (0.15 g, 0.1 mmol) was added to a stirred solution of $Mo(I)_2(CO)_3(NCMe)_2$ (0.103 g, 0.2 mmol) in THF (20 cm^3). The solid dissolved immediately to give a clear red–brown solution. After stirring further for 30 min to ensure complete reaction, the solution was filtered and the filtrate was concentrated to ca. 10 cm^3. Addition of hexane gave rise to a red–brown precipitate which was separated by filtration and purified by recrystallisation from acetone–ether to yield **5** (0.128 g, 53%). Anal. Calc. for $C_{80}H_{60}I_4Mo_2O_8P_4Pt_2S_2$: C, 39.6; H, 2.5; I, 20.9; Mo, 7.9; P, 5.1; Pt, 16.1; S, 2.6. Found: C, 39.6; H, 2.9; I, 19.0; Mo, 8.2; P, 4.9; Pt, 17.1; S, 2.8%. Λ_m (10^{-3} M, MeOH) 93 ohm^{-1} cm^2 mol^{-1}. δ_P (acetone-d_6) 19.7 (t, ^1J(P–Pt) = 3200 Hz).

Table 3
Crystallographic data for compounds **3a** and **3b**

	3a	**3b**
Chemical formula	$C_{88}H_{72}O_{16}P_4Pt_2Re_4S_2$	$C_{78}H_{66}BF_4O_4P_4Pt_2ReS_2$
M	2708.55	1918.50
Crystal system	Monoclinic	Monoclinic
Space group	$P2_1/c$	$P2_1/n$
Unit cell dimensions		
a (Å)	19.05(2)	17.054(4)
b (Å)	18.187(3)	23.826(4)
c (Å)	28.34(1)	18.452(4)
β (°)	96.93(3)	102.33(2)
V (Å^3)	9745(9)	7325(2)
Z	4	4
T (K)	293(2)	295(2)
μ (mm^{-1})	8.07	5.66
Crystal dimensions (mm)	$0.19\times0.19\times0.25$	$0.17\times0.33\times0.60$
Radiation	Graphite-monochromated Mo–K_α	Graphite-monochromated Mo–K_α
Scan mode	θ–2θ	θ–2θ
Absorption corrections	None	ψ-Scans
Min, max transmission	N/A	0.269, 0.996
Diffractometer	Nonius	Siemens P4
Max 2θ (°)	44.9	50.0
hkl Ranges	−20–20, 0–19, 0–30	−1–19, −1–28, −21–21
Reflections measured	13 182	14 637
Unique reflections (R_{int})	12 727 (0.083, based on F)	12 625 (0.062, based on F^2)
R_1 [a], wR [b]	0.105, 0.119 (R_w) [c] $[I>2.5\sigma(I)]$	0.057, 0.125 $[I>2\sigma(I)]$

[a] $R_1 = \Sigma||F_o|-|F_c||/\Sigma|F_o|$.
[b] $wR = [\Sigma w(F_o^2-F_c^2)^2/\Sigma w(F_o^2)^2]^{1/2}$.
[c] $R_w = [\Sigma w(|F_o|-|F_c|)^2/\Sigma w|F_o|^2]^{1/2}$.

3.6. Synthesis of $[Pt_2W(\mu_3\text{-}S)_2I(PPh_3)_4(CO)_4]X$ ($X = [W(I)_3(CO)_4]^-$, **6a**; $[PF_6]^-$, **6b**)

Complex **6a** was prepared in a manner analogous to **5** by reacting **1** (0.15 g, 0.1 mmol) with $[W(I)_2(CO)_3(NCMe)_2]$ (0.121 g, 0.2 mmol) in THF (20 cm^3) (yield 0.112 g, 43%). Anal. Calc. for $C_{80}H_{60}I_4O_8P_4Pt_2S_2W_2$: C, 36.9; H, 2.3; I, 19.5; P, 4.8; Pt, 15.0; S, 2.5. Found: C, 37.4; H, 2.5; I, 19.6; P, 4.2; Pt, 14.5; S, 2.2%. Λ_m (10^{-3} M, MeOH) 108 ohm^{-1} cm^2 mol^{-1}. δ_P (acetone-d_6) 19.6 (t, ^1J(P–Pt) = 3249 Hz).

$[Pt_2W(\mu_3\text{-}S)_2I(PPh_3)_4(CO)_4][PF_6]$ **6b** was prepared (isolated as a red–brown precipitate) by treating a solution of **6a** in MeOH with excess NH_4PF_6. Anal. Calc. for $C_{76}H_{60}F_6IO_4P_5Pt_2S_2W$: C, 44.1; H, 2.9. Found: C, 43.8; H, 2.5%. $\nu(PF_6^-)$ (KBr) 837 vs cm^{-1}.

3.7. Reaction of 1 with $[Mo(CO)_4(NCMe)_2]$

$Mo(CO)_6$ (0.037 g, 0.14 mmol) was refluxed in CH_3CN (10 cm^3) for 3 h to give a clear light brown solution of $[Mo(CO)_4(NCMe)_2]$. After the solution was cooled to r.t., **1** (0.15 g, 0.1 mmol) was added as a solid and the mixture stirred for 10 h to give a clear brown solution from which $[Pt_2(\mu\text{-}S)(PPh_3)_3(CO)]$ (**7**) (yield 0.019 g, 15%) was isolated by adding diethyl ether (50 cm^3) to facilitate precipitation. The complex was identified by its IR and ^{31}P-NMR spectra [28,29].

3.8. X-ray crystallography of complex 3a

Single crystals of complex **3a** were obtained by slow diffusion of hexane vapour into a solution of **3a** in Et_2O. Several crystals from different crystal-growing experiments were investigated, all of which were of irregular shape and did not diffract well. The crystal used for data collection gave only ca. 30% observed reflections with $I>2.5\sigma(I)$ (see Table 3).

The 3548 reflections with $I>2.5\sigma(I)$ were used for structure solution and refinement. The structure was solved by direct methods and difference Fourier maps. Structure refinement was hampered by the small number of observed reflections and disorder of the anion. The structure was refined to the isotropic convergence stage with only Pt, Re, S and P atoms allowed anisotropic motion. The refinement was performed with rigid-group constraints for each of the 12 phenyl rings

(excluding hydrogen atoms) of the cation, and the $\{Re_3(\mu\text{-}OC)_3(\mu_3\text{-}OC)\}$ fragment of the anion. In addition, the CO groups of the anion were constrained to shift simultaneously in the x, y and z directions. The Re_3 anion was disordered (ca. 90:10) with a second Re_3 anion. The major Re_3 cluster was modelled with an occupancy of 0.90 for each of the Re atoms and an occupancy 1.00 for each of the carbon and oxygen atoms. The minor Re_3 cluster was modelled with only three Re-atoms each with an occupancy of 0.10. An attempt to introduce hydrogen atoms in idealized positions did not improve the R-value.

The last least-squares cycle was calculated with 300 parameters and 3548 reflections. The weighting function used was $w^{-1} = \sigma^2(F_o) + 0.000100F_o^2$. The maximum shift/$\sigma$ ratio was 0.015. In the last difference map the highest peak was 2.42 e $Å^{-3}$ and the deepest hole was -3.03 e $Å^{-3}$. All calculations were performed on a Microvax 3600 computer with the NRCVAX system [33].

3.9. X-ray crystallography of complex **3b**

Single crystals of **3b** were grown by slow evaporation of a solution of the compound in acetone at r.t. The number of data used for structure solution and refinement was 7459 [$I > 2.0\sigma(I)$]. The structure was solved by direct methods. All non-hydrogen atoms, except for B(1), were refined anisotropically by the full-matrix least-squares method (on F^2). The $[BF_4]^-$ anion was refined with the constraints B–F = 1.390 ± 0.001 Å and F···F = 2.270 ± 0.001 Å. The latter constraint was introduced to fix the F–B–F angles at 109.5°. Hydrogen atoms were introduced in calculated positions and refined isotropically (riding model) in the final cycles of least-squares refinement. The Re–C≡O groups were constrained to be linear by requiring the Re···O distance for each Re–C≡O group to be equal (within ± 0.001 Å) to the sum of the corresponding Re–C and C–O bond lengths determined at anisotropic convergence. The last least-squares cycle was calculated with 860 parameters and 10 735 data (all of the unique reflections except the negative ones). The weighting function used was $w^{-1} = \sigma^2(F_o^2) + (0.0750P)^2$, where $P = (F_o^2 + 2F_c^2)/3$. The maximum shift/σ ratio was 0.005. In the last difference map the deepest hole was -1.322 e $Å^{-3}$, and the highest peak was 1.640 e $Å^{-3}$. Computations were carried out on a Pentium PC using the SHELXTL-PC software package [34].

4. Supplementary material

Crystallographic data for the structural analysis have been deposited with the Cambridge Crystallographic Data Centre, CCDC no. 133915 for **3a**, 133916 for **3b**.

Acknowledgements

This work was supported by the National University of Singapore (NUS) (RP 950695) and the National Institute of Education, Singapore (RP 15/95 YYK). H.L. and C.J. thank NUS for the award of a research scholarship. The authors acknowledge Professor Z. Lin of the Hong Kong University of Science and Technology for helpful discussions.

References

[1] H. Liu, A.L. Tan, K.F. Mok, T.S.A. Hor, Polyhedron 16 (1997) 337.
[2] (a) C.E. Briant, T.S.A. Hor, N.D. Howells, D.M.P. Mingos, J. Organomet. Chem. 256 (1983) C15. (b) H. Liu, A.L. Tan, C.R. Cheng, K.F. Mok, T.S.A. Hor, Inorg. Chem. 36 (1997) 2916.
[3] W. Bos, J.J. Bour, P.P.J. Schlebos, P. Hageman, W.P. Bosman, J.M.M. Smits, J.A.C. van Wietmarschen, P.T. Beurskens, Inorg. Chim. Acta 119 (1986) 141.
[4] C.E. Briant, T.S.A. Hor, N.D. Howells, D.M.P. Mingos, J. Chem. Soc. Chem. Commun. (1983) 1118.
[5] B.H. Aw, K.K. Looh, H.S.O. Chan, K.L. Tan, T.S.A. Hor, J. Chem. Soc. Dalton Trans. (1994) 3177.
[6] C.E. Briant, D.I. Gilmour, M.A. Luke, D.M.P. Mingos, J. Chem. Soc. Dalton Trans. (1985) 851.
[7] H. Liu, A.L. Tan, K.F. Mok, T.S.A. Hor, J. Chem. Soc. Dalton Trans. (1996) 4023.
[8] P.M.N. Low, Y.L. Yong, Y.K. Yan, T.S.A. Hor, S.-L. Lam, K.K. Chang, C. Wu, S.C.F. Au-Yeung, Y.-S. Wen, L.-K. Liu, Organometallics 15 (1996) 1369.
[9] Y.K. Yan, H.S.O. Chan, T.S.A. Hor, K.L. Tan, L.K. Liu, Y.S. Wen, J. Chem. Soc. Dalton Trans. (1992) 42.
[10] T.S.A. Hor, Y.K. Yan, Bull. Sing. N.I. Chem. 19 (1991) 115.
[11] J.E. Frazer, H. Hartley, Proc. R. Soc. London A 109 (1925) 351.
[12] S.-W.A. Fong, T.S.A. Hor, J. Chem. Soc. Dalton Trans. (1999) 639.
[13] P. Antognazza, T. Beringheli, G.D. Alfonso, A. Minoja, Organometallics 11 (1992) 1777.
[14] J. Xiao, J.J. Vittal, R.J. Puddephatt, L. Manojlovic-Muir, K.W. Muir, J. Am. Chem. Soc. 115 (1993) 7882.
[15] C. Jiang, Y.-S. Wen, L.-K. Liu, T.S.A. Hor, Y.K. Yan, Organometallics 17 (1998) 173.
[16] C. Jiang, Y.-S. Wen, L.-K. Liu, T.S.A. Hor, Y.K. Yan, J. Organomet. Chem. 543 (1997) 179.
[17] M.J. Calhorda, M.A.A.F. de C.T. Carrondo, A.R. Dias, V. Félix, A.M. Galvão, M.H. Garcia, P.M. Matias, M.J.V. de Brito, J. Organomet. Chem. 453 (1993) 231.
[18] (a) M.C. Durrant, D.L. Hughes, R.L. Richards, P.K. Baker, S.D. Harris, J. Chem. Soc. Dalton Trans. (1992) 3399. (b) P.K. Baker, M.C. Durrant, B. Goerdt, S.D. Harris, D.L. Hughes, R.L. Richards, J. Organomet. Chem. 469 (1994) C22.
[19] (a) P.K. Baker, S.G. Fraser, E.M. Keys, J. Organomet. Chem. 309 (1986) 319. (b) M.G.B. Drew, P.K. Baker, E.M. Armstrong, S.G. Fraser, D.J. Muldoon, Polyhedron 14 (1995) 617.
[20] P.K. Baker, S.G. Fraser, M.G.B. Drew, J. Chem. Soc. Dalton Trans. (1988) 2729.
[21] W.S. Tsang, D.W. Meek, A. Wojcicki, Inorg. Chem. 7 (1968) 1263.
[22] R. Colton, Coord. Chem. Rev. 6 (1971) 269.
[23] F.J. Arnaiz, G. Garcia, V. Riera, Y. Dromzée, Y. Jeannin, J. Chem. Soc. Dalton Trans. (1987) 819.
[24] M. Cano, J.A. Campo, M. Panizo, Polyhedron 16 (1997) 1095.

[25] K.-B. Shiu, K.-S. Liou, S.-L. Wang, S.-C. Wei, Organometallics 9 (1990) 669.
[26] (a) L. Bencze, A. Kraut-Vass, J. Mol. Catal. 28 (1985) 369. (b) L. Bencze, A. Kraut-Vass, L. Prókai, J. Chem. Soc. Chem. Commun. (1988) 911.
[27] M. Zhou, C.-F. Lam, K.F. Mok, P.-H. Leung, T.S.A. Hor, J. Organomet. Chem. 476 (1994) C32.
[28] C.-H. Chin, T.S.A. Hor, J. Organomet. Chem. 509 (1996) 101.
[29] M.C. Baird, G. Wilkinson, J. Chem. Soc. A (1967) 865. (b) A.C. Skapsi, P.G.H. Troughton, J. Chem. Soc. A (1969) 2772. (c) M. Hallam, M.A. Luke, D.M.P. Mingos, I.D. Williams, J. Organomet. Chem. 325 (1987) 271.
[30] R. Ugo, G. La Monica, S. Cenini, A. Segre, F. Conti, J. Chem. Soc. A (1971) 522.
[31] R.B. King, M.S. Saran, Inorg. Chem. 13 (1974) 74.
[32] E. Horn, M.R. Snow, Aust. J. Chem. 37 (1984) 1375.
[33] E.J. Gabe, Y. Le Page, J.-P. Charland, F.L. Lee, P.S. White, J. Appl. Crystallogr. 22 (1989) 384.
[34] G.M. Sheldrick, SHELXTL-PC, Version 5.03, Siemens Analytical X-ray Instruments Inc., Madison, WI, 1994.